View metadata, citation and similar papers at core.ac.uk
brought to you by CORE
provided by Elsevier - Publisher Connector

Available online at www.sciencedirect.com
SciVerse ScienceDirect
Energy Procedia 10 (2011) 261 – 265
Energy Procedia

European Materials Research Society Conference
Symp. Advanced Inorganic Materials and Concepts for Photovoltaics

Deep defects in Cu_2ZnSnS_4 monograin solar cells

E. Kask*, T. Raadik, M. Grossberg, R. Josepson, J. Krustok

Tallinn University of Technology, Ehitajate tee 5, Tallinn 19086, Estonia

Abstract

In this report Cu_2ZnSnS_4 (CZTS) monograin layer (MGL) solar cells were studied using admittance spectroscopy (AS) (frequency range 20Hz-10MHz) and temperature dependence of quantum efficiency (QE) curves (T=10K-300K). These studies revealed two deep defect states at E_{A1}= 120 meV and at E_{A2}= 167 meV. The first state was present in different CZTS cells while the second state had somewhat different properties in different cells. The temperature dependence of QE curves showed a shift of the long wavelength edge with increasing temperature by about 110 meV towards higher energy. The possible origin of the observed deep defect states is discussed.

© 2011 Published by Elsevier Ltd. Open access under CC BY-NC-ND license.

Selection and/or peer-review under responsibility of Organizers of European Materials Research Society (EMRS) Conference: Symposium on Advanced Inorganic Materials and Concepts for Photovoltaics.

Keywords: Cu_2ZnSnS_4; admittance spectroscopy; quantum efficiency; defects

1. Introduction

Cu_2ZnSnS_4 (CZTS) is a promising candidate for thin film solar cells with absorbers made from non-toxic and abundant elements [1-4]. At the same time it is very difficult to grow pure CZTS, because different secondary phases like ZnS, Cu_2SnS_3, and others are very easily formed and large compositional nonuniformity is present. This is a reason why even for such a fundamental parameter as the band gap energy agreement has not been reached: values between 1.4 eV and 1.6 eV have been reported [4-7]. Despite this fact the best solar cells based on CZTS have already shown efficiencies of almost 10 % [8]. However, without understanding the basic physical properties of CZTS it will be impossible to make a breakthrough similar to $CuInGaSe_2$ solar cells that show efficiencies of over 20 % [9].

It is known that intrinsic point defects in CZTS are playing a major role and determine the properties of CZTS. This is why more defect studies are needed. According to Losee [10], capacitance and admittance spectroscopy (AS) in particular are suitable methods for detecting defect levels. In defect studies also photoluminescence spectroscopy (PL) has proven to be a very efficient method. As far as we know there are no papers yet on capacitance spectroscopy studies of CZTS. So far only few papers about PL properties of CZTS have been published. A broad and asymmetric PL band at 1.3 eV has been detected in many papers [11-16]. Recently, even more PL peaks were detected in vapour phase grown CZTS crystals including a DA1 peak at 1.496 eV and a DA2 peak at 1.475 eV [12]. Both PL peaks are related to shallow defects with E < 30 meV. The first excitonic emission was also recorded in these crystals with a peak position at E=1.509 eV. From these measurements a low temperature (T=10K) band gap energy was calculated to

* Corresponding author. Tel.: +372-620-3210; fax: +372-620-3367.
E-mail address: erkki.kask@ttu.ee.

1876-6102© 2011 Published by Elsevier Ltd. Selection and/or peer-review under responsibility of Organizers of European Materials Research Society (EMRS) Conference: Symposium on Advanced Inorganic Materials and Concepts for Photovoltaics. Open access under CC BY-NC-ND license.
doi:10.1016/j.egypro.2011.10.188

be E_g=1.519 eV and the estimated room temperature band gap energy was 1.43 eV. In this paper we apply admittance spectroscopy and temperature dependent quantum efficiency (QE) measurements to study deep defects in CZTS solar cells.

2. Experimental

The CZTS monograin powder materials used for the solar cells studied were synthesized from binary compounds in a molten KI flux in an isothermal recrystallization process. The details of the monograin powder production process can be found in previous papers [4, 16]. The single phase composition of the monograin powder crystals was confirmed by Raman spectroscopy. The chemical composition was determined by energy dispersive X-ray analysis: Cu/(Zn+Sn)=0.9, Zn/Sn=1.1. Crystals with diameters of 63–75 μm were used in the formation of a monolayer in the monograin layer (MGL) solar cell structure: graphite/CZTS/CdS/ZnO [16]. The solar cells prepared have typically an area of about 4 mm^2.

We studied the solar cells by admittance spectroscopy. The solar cells were mounted on a cold finger of a closed-cycle helium cryostat (Janis) and a Wayne Kerr 6500B impedance analyzer was used for the electrical measurements. Impedance Z and phase angle θ were both measured as a functions of frequency f and temperature T. The used frequency range was from 20Hz to 10MHz and the temperature was varied from 95K to 300K with a step width ΔT of 5K. In order to maintain the linearity of the response signal, the alternating current (AC) voltage amplitude was kept as low as 10mV. The measurements were carried out in the dark and at 0V or -1V DC bias voltage.

For the temperature dependence of the QE curves a 250W calibrated halogen lamp was used as a light source together with a computer controlled SPM-2 prism monochromator. The temperature range was as wide as from 10K to 300K to find changes in the spectral response. The generated short circuit current was detected with a DSP Lock-In amplifier (SR 810).

I/V-measurements of CZTS cells were performed with a computer-controlled KEITHLEY 2400 SourceMeter at room temperature and under 100 mW/cm^2 illumination. As light source a standard halogen lamp with calibrated intensity was used.

3. Theory

Admittance spectroscopy involves measuring the junction capacitance as a function of frequency ω and temperature T. The admittance of the heterostructure is a superposition of the free carrier capacitance across the width of the space charge region (SCR) and the contribution from the charging and discharging of deeper defect levels within the SCR of the junction. The rectifying junction capacitance is given by the SCR capacitance [17]:

$$C_d = \frac{\varepsilon}{w} = \left(\frac{\varepsilon q N_a}{2V_{bi}}\right)^{1/2}, \quad (1)$$

where ε is the semiconductor's dielectric permittivity, w is the SCR width, N_a is the acceptor concentration in p-type absorber, and V_{bi} is the built-in voltage.

If deeper carrier traps are present, the band bending in the SCR causes the Fermi level E_F to cross the trap level E_t at some distance from the interface, at the crossing point x_t. The oscillating voltage with the frequency ω causes the electric charge accumulated by traps to oscillate in the vicinity of x_t. The trapped electric charge follows the applied voltage oscillations and contributes to the total capacitance only if their frequency does not exceed the characteristic trap frequency ω_t. Therefore, in the case of low frequencies $\omega_{lf} << \omega_t$, the trap related capacitance C_t is equal to C_{lf}, where C_{lf} is the low frequency capacitance. In high frequency ($\omega_{hf} >> \omega_t$) measurements the junction capacitance C_d is determined by C_{hf}, where C_{hf} is the high frequency capacitance. Accordingly, in the case of a single majority carrier trap level the total junction capacitance can be described by the equation [17]:

$$C(\omega) = C_d + \frac{C_{lf} - C_d}{1 + \omega^2 \tau^2}, \quad (2)$$

where τ is the characteristic trapping time that depends on the trap density N_t, the acceptor concentration N_a and on the SCR-width w. In the case of a small trap concentration N_t, the characteristic frequency ω_t for the hole trapping defects

is ω_t=1/τ [18]. The inflection frequency ω_t can be obtained from the analysis of the first derivative of the capacitance, $dC/d\omega$, that should demonstrate a peak at the frequency ω_t.

The temperature dependence of the inflection frequency ω_t is described by the equation [17]:

$$\omega_t(T) = 2e_t(T) = 2N_{c,v}\nu_{Th}\sigma_{n,p}\exp(-E_A/kT) = 2\xi_0 T^2 \exp(-E_A/kT), \quad (3)$$

where e_t is the emission rate, $N_{c,v}$ is the effective density of states in the conduction and valence band, υ_{Th} is the thermal velocity of the minority carriers at the interface, $\sigma_{n,p}$ is the capture cross-section for electrons and holes, E_A=E_t-E_v is the activation energy of the defect level E_t with respect to the valence band edge E_v in p-type absorber and ξ_0 covers all the temperature independent parameters. The activation energy of a defect level E_A can be obtained from the temperature dependence of the capacitance spectra i.e. from the Arrhenius plot of the quantity ln(ω_t/T^2) versus 1000/T.

4. Results and discussion

The *I-V* curve of our here most studied CZTS solar cell is given in Fig.1. As can be seen, this cell shows quite poor parameters: V_{oc}=582.4 mV, J_{sc}=7.13 mA/cm^2 and fill factor FF=32%, resulting in a solar energy conversion efficiency of only 1.3%. It is known that a low efficiency of CZTS cells is mainly caused by the high rate of interface recombination [19]. Additional recombination losses can be caused by deep acceptor levels that act as carrier traps. However, there are no experimental results about the deep defect levels in CZTS. Knowledge about the absorber surface properties and defect structure enables to improve the electrical properties of the CZTS material by changing the surface composition e.g. by the additional thermal and chemical treatments [4].

In order to study the defects in such CZTS powders, admittance spectroscopy was applied to CZTS MGL solar cells. Fig. 2 shows the frequency dependence of the capacitance of a CZTS solar cell in the temperature range from 95K to 300K. These spectra show two steps labelled N1 and N2 (similarly found for $CuInSe_2$ in [20]) that are attributed to the charging and discharging of two deep levels within the space charge region (SCR) of the heterojunction. The N2 capacitance step appears at lower frequencies and higher temperatures and corresponds therefore to a contribution of deeper defect level than N1. In accordance with the theory, the steps in the capacitance spectrum shift towards higher frequencies with increasing temperature T. The height of the capacitance steps corresponds to the defect level contribution to the total capacitance.

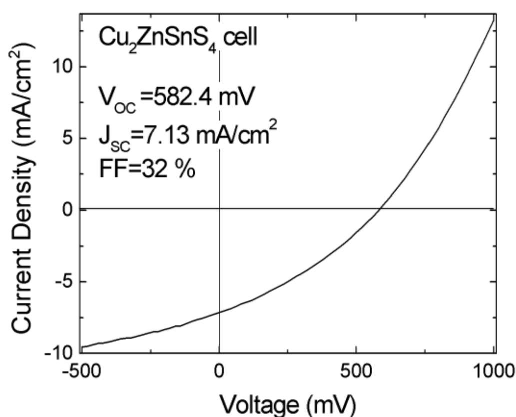

Fig. 1. Current-voltage characteristic of CZTS solar cell.

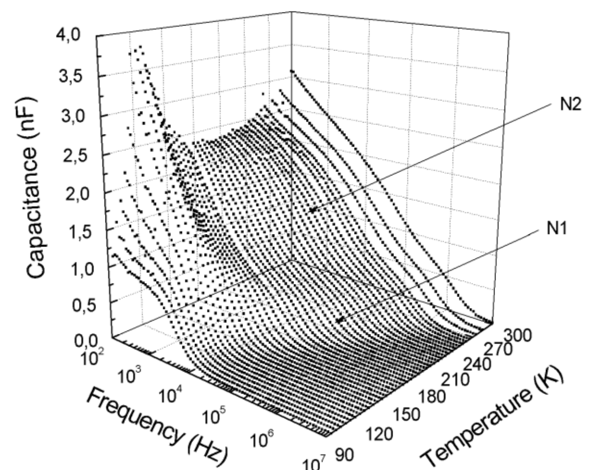

Fig. 2. The capacitance spectra of CZTS solar cell as a function of frequency and temperature at 0 V bias. Two steps, labelled N1 and N2 are indicated by arrows.

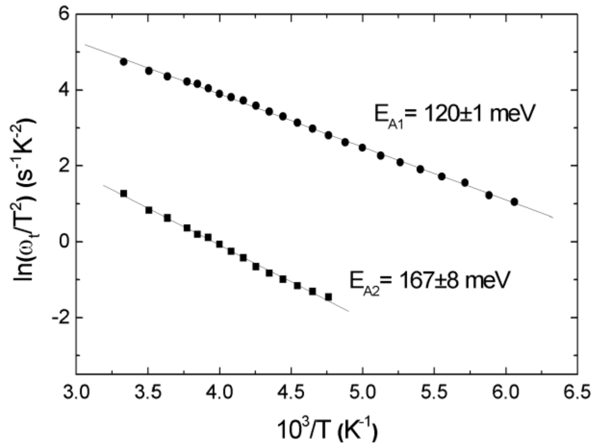

Fig. 3. The Arrhenius plot showing the calculated activation energies of the defect levels E_{A1}= 120 meV and E_{A2}= 167 meV corresponding to the two capacitance steps N1 and N2, respectively. Measured at bias 0 V.

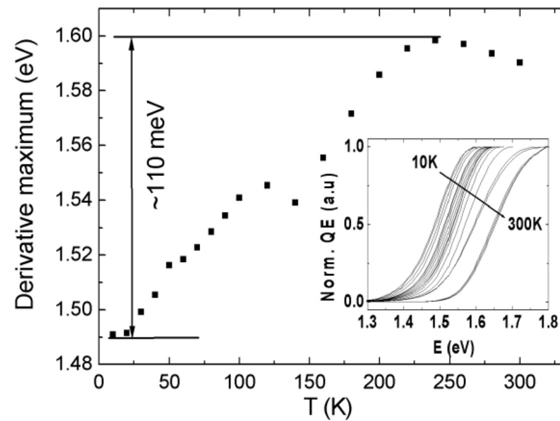

Fig. 4. Temperature dependence of the maximum points of the first derivative of the QE curves.

For the two capacitance steps, an Arrhenius plot of the quantity $\ln(\omega_t/T^2)$ versus $1000/T$ is shown in Fig. 3. The inflection frequencies ω_{t1} and ω_{t2} for every temperature corresponding to steps N1 and N2, respectively, were determined from the analysis of the first derivative $dC(\omega)/d\omega$. The obtained activation energies E_{A1}=120 ± 1 meV and E_{A2}=167 ± 8 meV are attributed to a defect distribution peaking at the corresponding energetic distance from the delocalized band edges.

The deep defect state with an activation energy of 120 meV was present in different CZTS solar cells while the second state with an activation energy of 167 meV had somewhat different properties in different cells. The activation energy of the latter defect state varied in different cells and was dependent on the applied bias voltage (0V, -1V). This is not expected for bulk defect states. On the other hand, in the case of reverse biasing the SCR is widened and the position of the interface states with respect to the Fermi level and the band edges changes. Consequently, we attributed the N2 capacitance step to the contribution of interface states.

The temperature dependence of the QE curves of the corresponding solar cells shows a shift of the long wavelength edge with increasing temperature by about 110 meV towards higher energy. Fig. 4 shows the maximum points of the first derivatives of the quantum efficiency (QE) curves at different temperatures. This shift seems to be related to the first defect state found from AS experiments. At low temperatures, this (probably acceptor) state contributes to the absorption and causes a shift of the QE curve. According to first-principles calculations made by Chen *et al*. [21] the *p*-type conductivity of CZTS is mainly determined by a Cu_{Zn} acceptor defect having a quite deep level at E_A= 0.12 eV. Accordingly, the deep acceptor level observed in AS measurements with the matching activation energy could be assigned to Cu_{Zn} acceptor defect.

5. Conclusions

Deep defects in CZTS monograin layer solar cells were studied by using admittance spectroscopy and temperature dependence of the quantum efficiency curves. The AS studies revealed two deep defect states at E_{A1}= 120 meV and at E_{A2}= 167 meV that were assigned to a Cu_{Zn} deep acceptor defect and to interface states, respectively. A shift in the temperature dependence of the quantum efficiency curves by about 110 meV towards higher energy was proposed to result from the contribution of this deep acceptor to the absorption at low temperatures.

Acknowledgements

This work was supported by the Estonian Science Foundation grant G-8282, by the target financing by HTM (Estonia) No. SF0140099s08, by European Social Fund's Doctoral Studies and Internationalisation Programme DoRa.

The support of the World Federation of Scientists National Scholarship Programme is gratefully acknowledged. The authors thank also the CZTSSe-team at the TUT.

References

[1] Katagiri H. Cu_2ZnSnS_4 thin film solar cells. Thin Solid Films 2005;**480-481**:426.
[2] Jimbo K, Kimura R, Kamimura T, Yamada S, Maw W S, Araki H, Oishi K, Katagiri H. Cu_2ZnSnS_4-type thin film solar cells using abundant materials. Thin Solid Films 2007;**515**:5997-5999.
[3] Katagiri H, Jimbo K, Maw W S, Oishi K, Yamazaki M, Araki H, Takeuchi A. Development of CZTS-based thin film solar cells. Thin Solid Films 2009;**517**:2455-2460.
[4] Mellikov E, Altosaar M, Raudoja J, Timmo K, Volobujeva O, Kauk M, Krustok J, Varema T, Grossberg M, Danilson M, Muska K, Ernits K, Lehner F, Meissner D. $Cu_2(Zn_xSn_{2-x})(S_yS_{1-y})_4$ monograin materials for photovoltaics. Materials Challenges in Alternative and Renewable Energy. Ceramic Transactions 2010;**224**:137-141.
[5] Katagiri H, Ishigaki N, Ishida T, Saito K. Characterization of Cu_2ZnSnS_4 Thin Films Prepared by Vapor Phase Sulfurization. Jpn. J. Appl. Phys. Part 1-Regular Pap. Short Notes Rev. Pap. 2001;**40**:500-504.
[6] Katagiri H, Saitoh K, Washio T, Shinohara H, Kurumadani T, Miyajima S. Development of thin film solar cell based on Cu_2ZnSnS_4 thin films. Sol. Energy Mater. Sol. Cells 2001;**65**:141-148.
[7] Fernandes P A, Salome P M P, da Cunha A F. Precursors' order effect on the properties of sulfurized Cu_2ZnSnS_4 thin films. Semicond. Sci. Technol. 2009;**24**:105013.
[8] Todorov T K, Reuter K B, Mitzi D B. High-efficiency solar cell with earth-abundant liquid-processed absorber. Adv. Mater. 2010;**22**:E156-E159.
[9] Jackson P, Hariskos D, Lotter E, Paetel S, Wuerz R, Menner R, Wischmann W, Powalla M. New world record efficiency for $Cu(In,Ga)Se_2$ thin-film solar cells beyond 20%. Prog. Photovolt: Res. Appl. 2011.
[10] Losee D L. Admittance spectroscopy of impurity levels in Schottky barriers. J. Appl. Phys. 1975;**46**:2204-2214.
[11] Tanaka K, Miyamoto Y, Uchiki H, Nakazawa K, Araki H. Donor-acceptor pair recombination luminescence from Cu_2ZnSnS_4 bulk single crystals. phys. stat. sol. 2006;**203**:2891-2896.
[12] Hönes K, Zscherpel E, Scragg J, Siebentritt S. Shallow defects in Cu_2ZnSnS_4. Physica B: Condensed Matter 2009;**404**:4949-4952.
[13] Oishi K, Saito G, Ebina K, Nagahashi M, Jimbo K, Maw W S, Katagiri H, Yamazaki M, Araki H, Takeuchi A. Growth of Cu_2ZnSnS_4 thin films on Si (100) substrates by multisource evaporation. Thin Solid Films 2008;**517**:1449-1452.
[14] Grossberg M, Krustok J, Raudoja J, Timmo K, Altosaar M, Raadik T. Photoluminescence and Raman study of $Cu_2ZnSn(Se_xS_{1-x})_4$ monograins for photovoltaic applications. Thin Solid Films (in press).
[15] Mellikov E, Altosaar M, Krunks M, Krustok J, Varema T, Volobujeva O, Grossberg M, Kaupmees L, Dedova T, Timmo K, Ernits K, Kois J, Oja Acik I, Danilson M, Bereznev S. Research in solar cell technologies at Tallinn University of Technology. Thin Solid Films 2008;**516**:7125-7134.
[16] Altosaar M, Raudoja J, Timmo K, Danilson M, Grossberg M, Krustok J, Mellikov E. $Cu_2Zn_{1-x}Cd_xSn(Se_{1-y}S_y)_4$ solid solutions as absorber materials for solar cells. phys. stat. sol. 2008;**205**:167-170.
[17] Bayhan H, Kavasoğlu A S. Admittance and Impedance Spectroscopy on $Cu(In,Ga)Se_2$ Solar Cells. Turk J Phys 2003;**27**:529-535.
[18] Gilmore A S, Kaydanov V, Ohno T R. The Study of Deep Levels in CdS/CdTe Solar Cells Using Admittance Spectroscopy and its Modifications. MRS Proceedings, Symposium B 2003.
[19] Wang K, Gunawan O, Todorov T, Shin B, Chey S J, Bojarczuk N A, Mitzi D, Guha S. Thermally evaporated Cu_2ZnSnS_4 solar cells. Applied Physics Letters 2010;**97**:143508.
[20] Herberholz R, Igalson M, Schock H W. Distinction between bulk and interface states in CuInSe2/CdS/ZnO by space charge spectroscopy. J. Appl. Phys. 1998;**83**:318-325.
[21] Chen S, Yang J-H, Gong X G, Walsh A, Wei S-H. Intrinsic point defects and complexes in the quaternary kesterite semiconductor Cu_2ZnSnS_4. Phys. Rev. B 2010;**81**:245204.